



21st European Conference on Fracture, ECF21, 20-24 June 2016, Catania, Italy

Fatigue analysis of adhesive joints with laser treated substrates

Fabrizio Moroni^{*a}, Marco Alfano^b, Luca Romoli^a

^aIndustrial Engineering Department, University of Parma, via G.P. Usberti 181/A 43124, Parma, Italy

^bDepartment of Mechanical, Energy and Management Engineering, University of Calabria, P. Bucci 44C, 87036, Rende (CS), Italy

Abstract

Recent literature works focused on the analysis of laser irradiation on the strength of adhesive joints under quasi-static loading conditions. It has been demonstrated that laser surface preparation allows to remove impurity and weak boundary layers from the mating substrates and, depending on the energy density, it is also able to modify surface morphology promoting mechanical interlocking. In previous works, the authors assessed the effect of Yb-fiber laser ablation over the quasi-static strength and toughness, of aluminum and stainless steel adhesively bonded joints. The experimental results demonstrated the ability of laser irradiation to improve the mechanical properties of the joints. The aim of this work is to extend the scope of previous investigations to fatigue loading. Double Cantilever Beam (DCB) samples with laser treated aluminum substrates have been bonded with a two component epoxy adhesive. For comparison standard degreasing and grit blasting have been also deployed for samples preparation. The results have been compared in terms of cycles to failure and the fracture surfaces have been analyzed by means of Scanning Electron Microscopy (SEM) in order to investigate the mechanism of failure.

Copyright © 2016 The Authors. Published by Elsevier B.V. This is an open access article under the CC BY-NC-ND license (<http://creativecommons.org/licenses/by-nc-nd/4.0/>).

Peer-review under responsibility of the Scientific Committee of ECF21.

Keywords: Adhesive Bonding, Laser Treatment, Fatigue Crack Growth

1. Introduction

Adhesive bonding is widely used in several industrial fields since it usually allows good mechanical performances, cost reduction and lightweight design if compared with traditional techniques. In general, the mechanical strength of a bonded joint depends on the strength of the adhesive itself (i.e. cohesive strength) and on the strength of the interface between the adhesive and the substrate (i.e. adhesive strength).

* Corresponding author. Tel.: +39 0521 905885

E-mail address: fabrizio.moroni@unipr.it

Nomenclature

P	Laser nominal power [W]
f	Lasing Pulse Frequency [kHz]
LS	Line spacing [μm]
d_S	Laser Spot Diameter [mm]
v	Lasing Speed [mm/s]
B	Joint Width [mm]
W	Joint Length [mm]
H	Substrate Thickness [mm]
t_a	Adhesive Thickness [mm]
a	Crack Length [mm]
a_0	Initial Crack Length [mm]
E_S	Substrate Young Modulus [MPa]
ν_S	Substrate Poisson Ratio
E_A	Adhesive Young Modulus [MPa]
ν_A	Adhesive Poisson Ratio
P_{max}	Maximum Load in a fatigue cycle [N]
P_{min}	Minimum Load in a fatigue cycle [N]
ΔP	Load Range in a fatigue cycle [N]
R	Load Ratio
δ	Opening measured by the omega clip gauge [mm]
G_{max}	Maximum Strain Energy Release Rate in a fatigue cycle [N/mm]
G_{min}	Minimum Strain Energy Release Rate in a fatigue cycle [N/mm]
ΔG	Strain Energy Release Rate Range in a fatigue cycle [N/mm]
λ_σ	Parameter of the Krenk (1992) model [mm^{-1}]
S_a	Surface Roughness [μm]

For a given adhesive, the joint strength can be improved by means of the several surface treatments that have been proposed in recent literature work, see for instance Alfano et al (2012), Chiodo et al (2014,2015) and Rotella et al (2016). These treatments aim to clean the surface by removing oxides and impurity and to induce modification in surface chemistry so that to achieve long-term durability.

Mechanical treatments usually consist of sand or grit blasting and their effectiveness on joint strength was evaluated for example by Mandolfino et al (2013). The variety of chemical treatments is instead wider, and the choice mainly depends on the kind of substrates selected for bonding. An overview of the available chemical treatments for aluminum substrates was provided by Critchlow and Brewis (1996).

However, these methods show a few drawbacks especially in terms of process control and repeatability, and from an environmental point of view (i.e. disposal of hazardous chemical waste). Therefore, cleaning and activation processes based on the use of plasma or laser beams represents nowadays a promising alternative to traditional methods. The effect of laser ablation over the quasi-static strength of bonded joints was investigated by Rechner et al (2010), Kim et al (2010), Wong et al (1997) Alfano et al (2012), Chiodo et al (2014, 2015). It was observed that laser ablation enhances the adhesion strength by removing impurity and promoting mechanical interlocking. However, several works analyzed the joint behavior under quasi-static loading while the effect of cyclic fatigue loading received less attention.

This work aims to fill this gap and is devoted to the characterization of the mode I fatigue resistance of adhesive bonded aluminum Double Cantilever Beam (DCB) bonded joints before and after laser surface irradiation. In particular, for comparison grit blasted and degreased joints were also prepared and tested in order to understand the effectiveness of the laser treatment. The results were compared in terms of fatigue crack growth rate as a function of the applied range of strain energy release rate.

2. Surface preparation

Laser treatment consists in laser radiation of a surface: the pulsed laser beam is focused on the surface and produces a high density energy radiation. Depending on the power of the radiation, the laser can produce a surface cleaning (low power) by removing oxides and impurities, or, a morphological modification of the surface (high power) produced by the localized melting, or vaporization, of a thin external layer of the material.

In this work, laser ablation was performed using a LaserPoint YFL 20P pulse ytterbium fiber laser, equipped with galvanometer lens, used for the laser beam motion. By leveraging on the authors previous works (Chiodo et al 2014, 2015), the treatment was herein carried out by using a pulse frequency (f) equal to 20kHz, and an average power (P) equal to 20W. The spot size (d_s) was equal to 0.035mm, and it was moved along parallel lines having a pitch (LS) of 0.07mm. Two laser scanning speeds (v) were evaluated: 5mm/s and 50mm/s; higher speeds are indeed more appealing from an industrial point of view because of the reduced amount of time needed to complete the treatment.

Laser irradiation induces surface morphological modifications, such as the trench-like grooves which are reported in the optical microscopy images reported in Fig. 1. For comparison purpose also grit blasted and simple degreasing, using Loctite 7063 (a general purpose solvent-based degreaser), specimens were prepared. The roughness of the surface was measured for each surface condition. The values of measured S_a are shown in Table 1.

The treatments were carried out in air and at room temperature and the substrates were bonded within 1 hour from completion of the treatment.

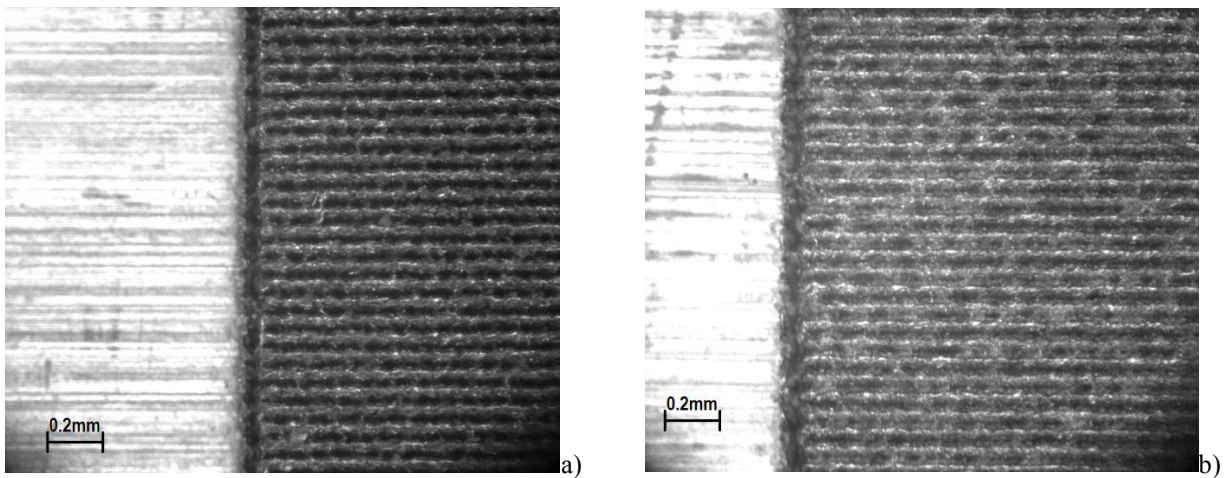


Fig. 1. Example of a laser ablated aluminum surfaces: a) treated at 5mm/s b) treated at 50mm/s.

Table 1. Surface Roughness of treated Substrates

Surface Condition	S_a [μm]
Laser Treated (5mm/s)	9.01
Laser Treated (50mm/s)	7.08
Grit Blasted	5.68
Degreased	1.82

3. Sample fabrication, testing and data reduction scheme

In order to characterize the mode I crack growth fatigue strength of laser treated, grit blasted and degreased bonded joints, fatigue tests were carried out on aluminum (AA 6082 T4) DCB specimens, bonded using Loctite Hysol 9466, a two component adhesive. Fig. 2 shows the joint geometry. Table 2 and Table 3 respectively show the

specimen dimensions as well as the substrate and adhesive mechanical properties. Adhesive curing was performed at 80°C for 60 minutes. The adhesive thickness was controlled by means of spacer placed at two ends of the joint. The initial crack length was set by mean of a thin Teflon layer placed between the two substrates.

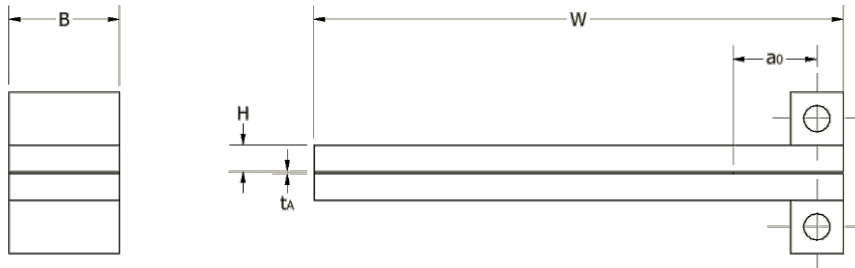


Fig. 2. Sample dimensions.

Table 2. Specimen dimensions.

Symbol	Dimension	Value
W	Width [mm]	120
B	Depth [mm]	25
H	Adherent Thickness [mm]	6
t_A	Adhesive Thickness [mm]	0.1
a_0	Initial crack length (nominal) [mm]	25

Table 3. Material Properties.

Symbol	Dimension	Value
E_S	Substrate Young Modulus [MPa]	70000
ν_S	Substrate Poisson ratio	0.3
E_A	Adhesive Young Modulus [MPa]	1700
ν_A	Adhesive Poisson ratio	0.33

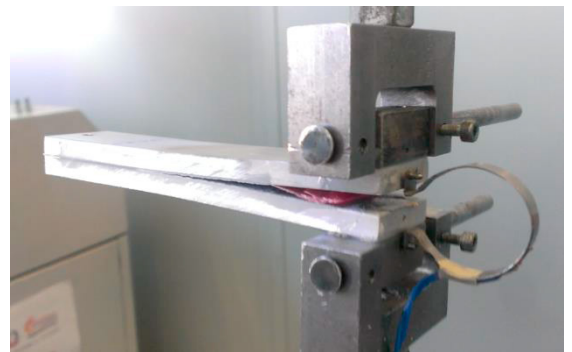
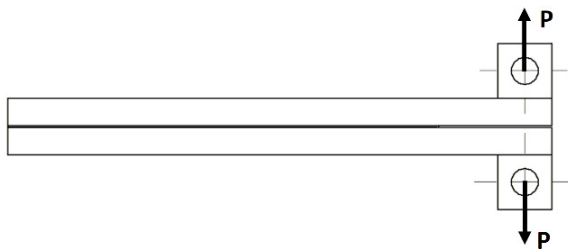


Fig. 3. Loading set-up and detail of the clip gauge employed to track the crack-opening during testing.

Mode I fatigue tests were carried out using the set-up shown in Fig. 3. The specimens were initially pre-cracked in order to achieve a non-artificial crack tip, and later subjected to fatigue loading. Fatigue tests were conducted at constant load ratio $R = P_{min}/P_{max} = 0.1$ and at constant load amplitude $\Delta P = P_{max} - P_{min}$. The testing frequency was set to

5Hz. The crack length was monitored by means of the compliance method. The crack opening (δ) was measured by means of a clip gauge (Fig. 3). The relationship between the compliance (δ/P) and the crack length (a) was obtained by means of finite element simulations carried out at different crack lengths (Fig. 4). This relationship was then used to obtain the crack length by tracking the experimental compliance during the test.

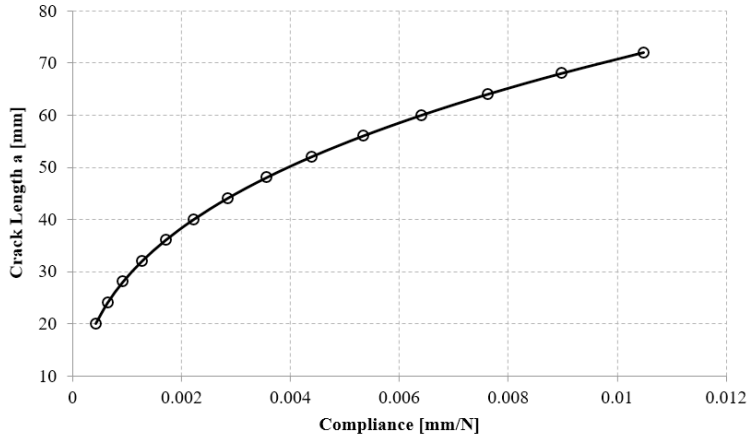


Fig. 4. Compliance vs Crack length obtained through finite element simulations.

The test results are presented in terms of crack growth rate as a function of the range of the applied strain energy release rate (ΔG). For a DCB joint the strain energy release can be obtained using the relationship proposed by Krenk (1992), and in particular, the maximum value achieved within a load cycle is given by:

$$G_{\max} = \frac{12(P_{\max} a)^2}{B^2 E_S H^3} \left(1 + \frac{1}{\lambda_{\sigma} a} \right)^2 \tag{1}$$

where:

$$\lambda_{\sigma} = \sqrt[4]{\frac{6E_A}{H^3 t_A E_S (1-\nu_A)^2}} \tag{2}$$

The range of the strain energy release rate is defined as:

$$\Delta G = G_{\max} - G_{\min} \tag{3}$$

therefore by using the load ratio definition, ΔG can be computed as:

$$\Delta G = G_{\max} (1 - R^2) = \frac{12(P_{\max} a)^2}{B^2 E_S H^3} \left(1 + \frac{1}{\lambda_{\sigma} a} \right)^2 (1 - R^2) \tag{4}$$

4. Results

The results of the fatigue tests are shown in Fig. 5. It is apparent that grit blasted specimens display crack growth rates significantly lower with respect to the degreased ones. Concerning the laser treated specimens, it can be noticed that they are characterized by a crack growth rate that is rather similar to that observed on the grit blasted specimen.

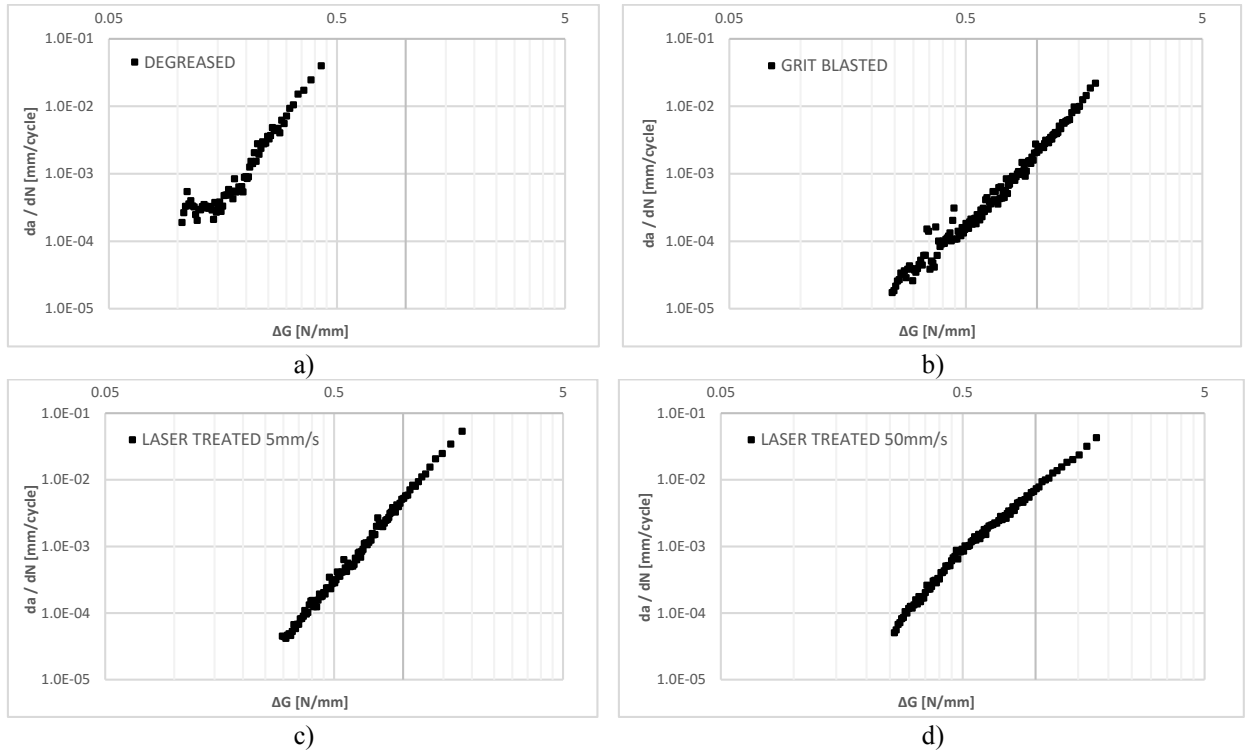


Fig. 5. Result of fatigue test for a) degreased, b) grit blasted, c) laser treated at 5mm/s and d) laser treated at 50mm/s.

For each plot a regression to a power law is carried out in order to obtain the coefficients of the Paris equation (Eq. 5):

$$\frac{da}{dN} = C(\Delta G)^m \tag{5}$$

The so obtained coefficients are provided in Tab. 4. It can be noticed that the slopes of the regression curves are similar to each other, while significant differences are shown in term of the intercept C: for the degreased specimen this value is two order of magnitude higher than the other, while it is quite similar for laser treated and grit blasted joints.

In order to analyze more in detail the results of fatigue tests, a survey of the fracture surfaces was made by using both optical microscopy and scanning electron microscopy. It is worth noting that when subjected to cyclic loading, fatigue cracks can initiate in the adhesive or at the adhesive/adherent interface. These cracks can propagate and eventually cause failure of the bonds. Fig. 6 shows the typical failure surface morphologies observed on DCB samples subjected to fatigue loading. The visual inspection indicates that degreased sample undergone near interfacial failure (adhesive failure) and that the failure path shifted from one interface to the other in irregular

fashion. It is also apparent that grit blasting as well as laser surface irradiation led to cohesive fracture within the adhesive layer.

Table 4. Material Properties.

Surface Condition	C [$\text{mm}^{\text{m}+1}\text{N}^{\text{m}}\text{cycle}^{-1}$]	m
Laser Treated (5mm/s)	$4.9 \cdot 10^{-3}$	4.03
Laser Treated (50mm/s)	$7.6 \cdot 10^{-3}$	3.39
Grit Blasted	$2.0 \cdot 10^{-3}$	3.37
Degreased	$5.7 \cdot 10^{-1}$	3.75

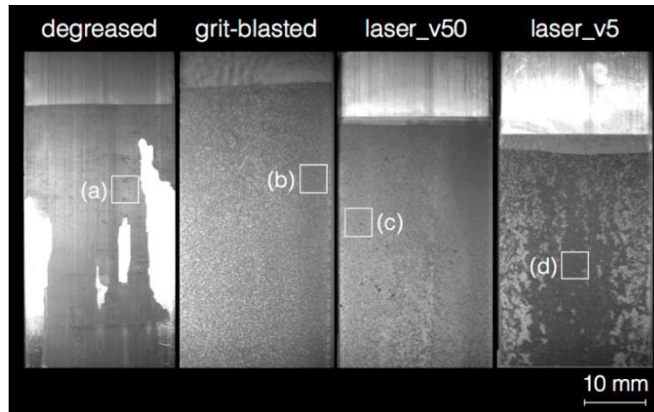


Fig. 6. Visual observation of the fracture surfaces as a function of the surface preparation method. The squares indicate the approximate locations where the samples for SEM analyses were taken. Failure was adhesive for degreased samples, while it was cohesive for grit-blasted and laser treated samples.

However, some differences can be observed. Laser treatment at higher speed, 50 mm/s, induced the formation of fractured surfaces seemingly identical to those observed on grit-blasted samples. However, when the laser was operated at low speed the appearance of the fractured surfaces was no longer similar, since the crack ran much closer to one of the interface, especially near the edges of the substrates. The observed differences among the various failure modes testify the important effect of surface conditions on the failure behavior. While the initial featureless surface of degreased samples led to essentially adhesive failure, after sand blasting and laser irradiation the crack path was shifted within the adhesive layer. It can be concluded that the induced surface roughness promoted mechanical interlocking and resulted in cohesive failure within the bondline.

SEM analyses were also carried out and are reported in Fig. 7. Fig. 7(a) shows the appearance of the fracture surfaces of degreased samples. The crack path shifted from one interface to the other uncovering the underlying bare substrate. It is worth noting that at present time we did not perform EDX analyses to precisely determine if there is any trace of adhesive left on the interface. In the remaining cases cohesive failure was clearly observed. The most striking feature of Fig. 7(b-d) is the amount of entrapped air that was found in the adhesive layer. It is speculated that the air entrapped within the asperities of the substrates during adhesive dispensing is subsequently transferred within the bondline following adhesive curing at high temperature. The amount of air voids was greater at lower laser scanning speed. This is probably associated to the greater extent of the surface morphological modifications induced by the laser at lower speed. In fact, low scanning speed implies a higher interaction time between the laser beam and the target surface. As a result, deeper cavities are created, and because of the gap filling capabilities of the adhesive higher amount of air can be entrapped at the interface.

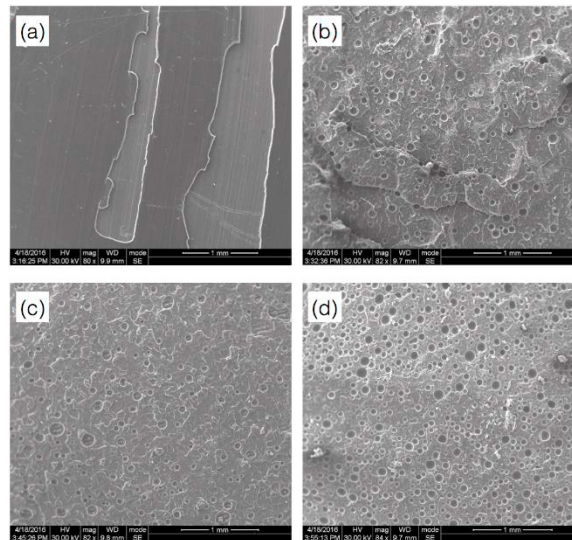


Fig. 7. SEM observations of selected failed surfaces as a function of surface conditions. (a) Degreased; (b) grit-blasted; (c) laser treated at 50 mm/s; (d) laser treated at 5 mm/s. The appearance of the fractured surfaces testifies that failure was adhesive for degreased samples, while it was cohesive for all the remaining conditions.

5. Conclusion

In the present paper the effect of laser treatment on the mode I fatigue crack growth of aluminum bonded joint was analyzed. The results testify that the modifications induced by laser irradiation enabled the development of an improved interfacial strength and induced fatigue crack growth within the bondline. Therefore, laser irradiation not only improves the joint strength under static condition, but it also enhances the mechanical behavior under cyclic fatigue loading.

References

- Alfano M, Lubineau G, Furgiuele F, Paulino G H, 2012. Study on the role of laser surface irradiation on damage and decohesion of Al/epoxy joints, *International Journal of Adhesion & Adhesives* 39, 33–41.
- Chiodo G, Alfano M, Pini S, Pirondi A, Furgiuele F, and Groppetti R. 2014 Double cantilever beam testing of Al/epoxy joints with low power laser treated substrates. *Procedia Materials Science* 3, 1479 – 1484.
- Chiodo G, Alfano M, Pini S, Pirondi A, Furgiuele F, and Groppetti R. 2015 On the effect of pulsed laser ablation on shear strength and mode I fracture toughness of al/epoxy adhesive joints. *Journal of Adhesion Science and Technology* 29(17), 1820-1830.
- Critchlow G, Brewis D, 1996 Review of surface pretreatments for aluminium alloys, *International Journal of Adhesion & Adhesives* 16(4), 255-276
- Kim W.S., Yun I.H., Lee J.J., Jung H.T., 2010 Evaluation of mechanical interlock effect on adhesion strength of polymer–metal interfaces using micro-patterned surface topography. *International Journal of Adhesion & Adhesives* 30, 408–417
- Krenk S, 1992 Energy Release Rate of Symmetric adhesive joints, *Engineering Fracture Mechanics* 43, 549-559
- Mandolfino C, Lertora E, Gambaro C, 2013 Effect of Surface Pretreatment on the Performance of Adhesive-Bonded Joints, *Key Engineering Materials*; 554-557: 996-100
- Rechner R, Jansen I, Beyer E, 2010 Influence on the strength and aging resistance of aluminium joints by laser pre-treatment and surface modification. *International Journal of Adhesion & Adhesives* 30, 595–601
- Rotella G, Alfano M, Schiefer T, Jansen I, 2016. Evaluation of mechanical and laser surface pre-treatments on the strength of adhesive bonded steel joints for the automotive industry, *Journal of Adhesion Science and Technology* 30(7), 747-758.
- Wong RCP, Hoult AP, Kim JK and Yu TX, 1997 Improvement of adhesive bonding in aluminium alloys using a laser surface texturing process. *Journal of Materials Processing Technology* 63, 579-584